

This document is the Accepted Manuscript version of a Published Work that appeared in final form in *Analytical Chemistry*, copyright © American Chemical Society after peer review and technical editing by the publisher. To access the final edited and published work see <http://pubs.acs.org/doi/10.1021/acs.analchem.5b02239>

Numerical modeling of solid phase microextraction focused on uptake kinetics

Md. Nazmul Alam¹, Luis Ricardez-Sandoval², Janusz Pawliszyn^{1*},

^{1*}Department of Chemistry, University of Waterloo, Waterloo, Ontario, N2L 3G1, Canada

²Dept. of Chemical Engineering, University of Waterloo, Waterloo, N2L 3G1, Canada

Phone: 1-519-888-4567 ext. 84641. Fax: 1-519-746-0435. E-mail:

janusz@sciborg.uwaterloo.ca

Abstracts

Solid phase microextraction (SPME) is a well-known sampling and sample preparation technique used for a wide variety of analytical applications. As there are various complex processes taking place at the time of extraction that influence the parameters of optimum extraction, a mathematical model and computational simulation describing the SPME process is required for experimentalists to understand and implement the technique without performing multiple costly and time-consuming experiments in the laboratory. In this study, a mechanistic mathematical model for the processes occurring in SPME extraction of analyte(s) from an aqueous sample medium is presented. The proposed mechanistic model was validated with previously reported experimental data from three different sources. Several key factors that affect the extraction kinetics, such as sample agitation, fiber coating thickness, and the presence of other undesirable species (matrix), are discussed. More interestingly, for the first time, enhancement or retardation of extraction kinetics in the presence of the matrix were explained with the help of an asymptotic analysis. The parameters that contribute to the different types of observed matrix effects on the uptake kinetics are also discussed. Numerical simulation results show that the proposed model captures the phenomena occurring in SPME, leading to a clearer understanding of this process. Therefore, the currently presented model can be used to identify optimum experimental parameters without the need to perform a large number of experiments in the laboratory.

.....

Key words: solid phase microextraction, mathematical model, numerical simulation, matrix effects

Introduction

Solid phase microextraction (SPME) has already been recognized by the scientific and industrial community as a powerful alternative sampling and sample preparation technique to technologies such as liquid-liquid or solid phase extraction, as is evidenced by its rapid growth over the past decades.¹ The theory and practice of SPME have been examined in considerable detail in recent years in order to facilitate the processes of learning and application of this relatively new technique.² In SPME, a small amount of extracting material (usually polymeric) is dispersed onto a solid support to create an open-bed extraction phase. When the solid-supported extraction media is exposed to an analytical sample for a period of time, the extraction yield is primarily dependent on the partitioning of analyte(s) between the sample bulk phase and the supported extraction phase. The partitioning is in turn dominated by the physicochemical factors related to the analyte, the sample matrix (i.e., the part of sample other than the analyte), and the extraction phase. Based on the total residence time of the extraction phase in the sample solution, two extraction methods are used: (i) equilibrium extraction, which refers to extractions that take place when the extraction amount does not change significantly, or when partition equilibrium is reached and, (ii) non-equilibrium extraction, which is the extracted amount at any given time before a state of equilibrium is reached. The extraction processes in SPME consist of several physical domains with several processes occurring simultaneously, i.e., diffusion, convection, matrix binding, and adsorption or absorption.³ Different research groups have proposed slightly different approaches to model the kinetics of the absorption process for SPME. For example, some groups^{4,5} considered the SPME fiber as a one-compartment, first-order kinetic model, whereas our group² divided the uptake process into two parts: intra-fiber molecular diffusion in

the coating domain, and mass transfer around the fiber, which is governed by intra-layer molecular diffusion over a stagnant layer with a finite thickness. Hermens' group modified the later approach by introducing the mass transfer coefficient as a leading force due to the concentration gradient between the bulk medium and the fiber surface.⁶ Nevertheless, all these models have been simplified such that an analytical solution for the proposed model can be obtained; this can cause difficulties for experimentalists seeking to implement them in developing practical SPME methods that can be realistically applied to actual systems. Moreover, quantification of freely dissolved analytes with SPME under non-equilibrium conditions can be erroneous due to the influence of matrix components in the kinetic regime of extraction.⁷ Some studies reported an increased analyte uptake rate in the presence of matrix during the kinetic phase of extraction.⁸ The plausible explanation for this enhanced kinetics is known as the "diffusion layer effect".⁷ Conversely, other studies reported unaltered uptake kinetics in the presence of matrix.⁹ Although the majority of the reports agree with the fact that the matrix can affect the uptake kinetics only if the extraction is limited by the diffusion in the boundary layer, a lack of understanding remains regarding the effect of the physical parameters on the transport kinetics in a complex matrix.

In spite of all the developments achieved in different aspects of SPME, from the creation of different formats to its expansion of applications, it still remains a challenge for experimentalists to readily determine suitable experimental conditions that can provide acceptable (optimal) extraction amounts at low analyte concentrations. As such, the development of a computational model will help increase our current knowledge of SPME methods by providing insight into the nature and dynamic characteristics of the extraction process. Computational modeling and theoretical simulation have become very important tools for the

development of analytical microsystems such as microfluidics and sensors.¹⁰ In addition, the design of suitable devices for SPME, as well as method development for different applications, can be a laborious undertaking, since a number of parameters need to be optimized for a given set of analyses. Hence, the utilization of a computational model would significantly decrease the time and labor needed to develop and test several SPME designs as compared to the current practice of performing multiple (expensive) experiments.

In this work, a computational-based mechanistic model for the absorption processes occurring in SPME has been developed using the finite element analysis software, COMSOL MULTIPHYSICS™. Several common SPME experimental parameters, such as fiber coating thickness, analyte concentration, and the matrix effect were considered and tested with the proposed model. The mechanistic model presented in this study is able to provide insight into how physical parameters affect the extraction kinetics of an analyte from a matrix-containing sample. A set of general guiding principles that were adapted from an asymptotic analysis¹¹ were used as a predictive tool to achieve desired uptake kinetics or to explain the experimental extraction time profile for a complex matrix. The mechanistic model was validated with previously published experimental data obtained from different sources.

Experimental Section

Mathematical model

The present model involves three simultaneous and coupled processes: fluid flow past the SPME fiber dipped in the sample to be analyzed, mass transport to and from the fiber coating, and absorption of analyte by the fiber coating. Each of the domains considered in the present model is described next.

In the present mechanistic model, a typical geometry of SPME sampling was set up based on the experimental configurations reported by Louch et al.,¹² where the sample was placed in a vial stirred with a magnetic stirrer, which provided convective flow, and the SPME fiber was inserted through the vial cap. A schematic representation of the sample vial and SPME fiber, along with the corresponding modeling domain, is depicted in Figure 1(a). The fiber was located away from the center of the vial in order to avoid the central vortex region and to satisfy the assumption that the fluid flows past the fiber with a velocity normal to the fiber axis.¹³ The present analysis assumes a simple 2D geometry (Figure 1(b)) for simplicity of modeling and in order to reduce the amount of necessary calculations. The xy plane is set to be the cross-section of the sample container, whereas the x-axis is set to be along the direction of flow. The governing equations for the fluid flow, the mass transport, and the matrix effect are described next.

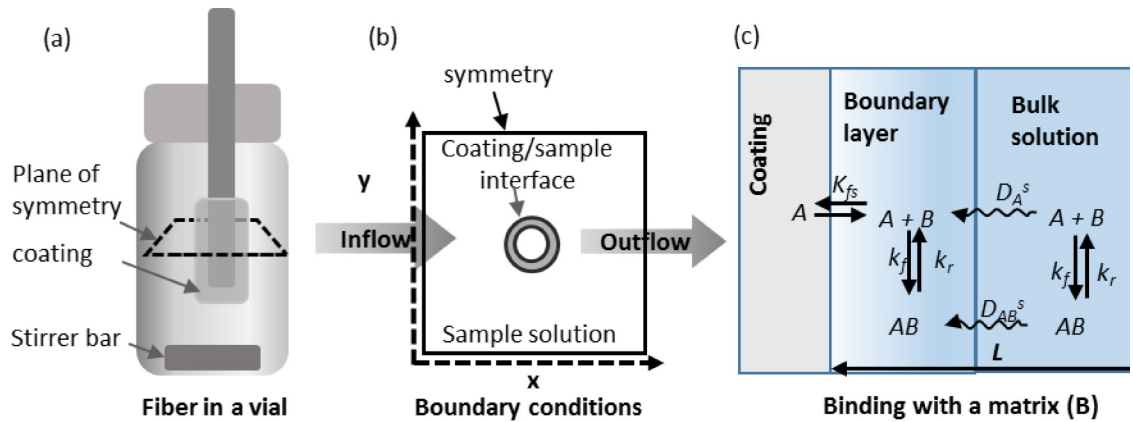


Figure 1. Schematic representation of the SPME/sample configuration. Experimental geometry based on Louch et al. containing a magnetic stirrer mediated convection, (a).¹² Here, a silica rod is used as a support for the coating, which is immersed in a sample solution for direct extraction. The 2D geometry with the boundary conditions used in the model, (b). A schematic diagram of the transport processes occurring in each region in the presence of matrix (B), (c). An analyte (A) binds with a matrix (B) with forward and reverse rate constants (k_f) and (k_r), respectively. Both the free or bound analytes can diffuse to the boundary layer with diffusivities D_A^s and D_{AB}^s , respectively. On the coating, only the analyte can be absorbed with a distribution constant of K_{fs} .

Fluid flow equations

Since the flow in the sampling container of SPME is in a low Reynolds number condition, it is assumed to be a laminar flow. The Navier-Stokes equation was employed to model the fluid flow in the sampling container. The conservation of momentum for incompressible fluid flow in a 2D geometry can be formulated as follows:

$$(1)$$

$$(2)$$

Where u and v are the velocity components in the x and y directions, respectively; ρ is the fluid density, p is pressure and μ is the fluid viscosity. For incompressible fluid flows, the following continuity equation is also considered:

$$(3)$$

The boundary conditions for the fluid flow model are shown in Figure 1(b). Symmetry conditions were set at the two edges (Figure 1(b)). The boundary condition at the outlet was set to $p = 0$. A linear velocity was set at the inlet of the geometry. In order to obtain the linear velocity from stirring the solution with a magnetic stir bar, the following equation was employed:

2

$$(4)$$

Where R is the radius of the stir bar and N represents the revolutions per second.

Mass transport equations

The analyte is transported by diffusion and convection in the bulk solution, whereas diffusion is the only transport mechanism occurring in the fiber coating. According to Fick's law,

the following mass balances can be formulated to describe the time-dependent mass transport model for the present system¹⁴:

$$(5)$$

$$(6)$$

Where C_A^s and C_A^f denote the concentrations (mol m^{-3}) of the analyte A in the solution phase and fiber coating, respectively. D_A^s is the diffusivity coefficient (m^2s^{-1}) in the solution phase, and D_A^f is the diffusivity coefficient in the fiber coating, while \mathbf{U} denotes the velocity field, which can be obtained from the Navier-Stokes model described in the previous section. Equation (5) is valid for the solution side where convection is applied, whereas equation (6) is for the fiber's domain, where only diffusion is assumed to occur. At the coating/solution boundary, the conditions that ensure continuity of the dependent variables in the two regions, i.e., fiber coating and aqueous solution, need to be specified.¹⁵ This specification is needed due to the nature of the analyte concentrations found at these two sites; while there is normally a movement of mass flux across the boundary, the overall concentration is most often discontinuous, since the individual concentrations on the coating and in the solution are different from each other (the boundary condition is schematically shown in the supplementary information in Figure S1). To circumvent this issue, two separate concentrations, i.e. concentration on the solution side (C_A^s) and on the fiber side (C_A^f), have been specified. Then, the concentrations are coupled using an equilibrium relationship, i.e., a partition coefficient ($K_{fs} = C_A^f/C_A^s$). When a liquid phase is in contact with a solid phase, the K_{fs} can be defined as the ratio of the concentration of a species in the solid phase to that in the liquid phase where they come in contact.² The fluxes are then coupled using Newton's law type expressions:

$$(7)$$

(8)

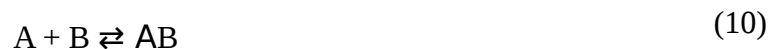
Where M is an arbitrary parameter called the stiff-spring velocity term, which should be of a large enough value so that a considerable mass exchange between the two regions can be established. In the present analysis, the value of M was considered as 1000 m/s, since it provided sufficient mass exchange at the coating/solution interface. This technique has been used in previous studies that consider mass transfer between two different media.^{16,17}

A specified inlet concentration equal to the initial concentration was set at the inlet boundary ($C_A^s = C_A^{s,0}$) and vanishing of $\frac{\partial C_A^s}{\partial x}$ at the outlet. The following equality of the mass flux of the analyte was considered at the sample vessel wall:

(9)

Binding matrix

When a binding matrix is present, (e.g., humic organic matter in a water sample), the association and dissociation between the freely dissolved analytes and the binding matrix in the sample domain can be expressed as follows:



Where A is the freely dissolved analyte, B represents the binding matrix, and AB is the bound species. The present study assumes that the fiber coating absorbs only analytes in a matrix-containing sample and follows the same physics as described in the previous section. In the solution domain, simple binding kinetics between analyte and matrix were used to model the influence of the matrix on the extraction of analyte (i.e. second-order forward and first-order

backward).¹⁸ As the main objective to this work was to develop an integrated mechanistic mathematical model and computational simulation that describes the effect of matrix on kinetics of extraction, the effect of fiber coating damage by adsorption or partition of matrix components is not considered. The modeled experimental systems involved addition of bovine serum albumin or humic acids to water samples, as previously reported in the literature.^{19,20} The model parameters used in this study are shown in Table S1, found in the supplementary information. The transport of the species in the sample is schematically shown in Figure 1(c).

The rates of association (k_f) and dissociation (k_r), commonly expressed as the dissociation constant (K_D), determine the strength of the affinity interaction (Equation (11)), which regulates analyte release from the bound matrix into the sample media.

(11)

Here, C_A , C_B , and C_{AB} are the molar concentrations of the free analyte in the sample matrix, the uncomplexed or free matrix (e.g., humic acid), and the complexed or bound matrix, respectively.

The mass transport within the sample matrix can be described using mass balances for the analyte and the bound matrix. The concentration of free analyte (C_A) at the diffusion boundary layer changes in relation to the diffusion from the sample matrix, as well as association or dissociation with the bound matrix, i.e.,

(12)

where $C_{B,T}$ is the concentration of total matrix added.

The concentration of complex (C_{AB}) relies only on the equilibrium binding,

(1
3)

where the concentration of free binding matrix (C_B) is described as the difference between the concentration of total matrix added ($C_{B,T}$) and the concentration of complex (C_{AB}), i.e.,

(1
4)

Computational model

COMSOL Multiphysics 4.4, a finite element method (FEM) based software package, was used in this study to analyze the mass transfer processes in SPME. In order to obtain an accurate representation of the SPME system, the time-dependent partial differential equations for each of these physical processes must be solved simultaneously. The procedure used to solve this problem is divided into two steps: (1) determination of the fluid velocity profile at steady-state assuming incompressible flow and (2) use of this steady-state velocity profile as the initial condition to solve for the coupled transient mass transport and absorption equations.

Results and Discussions

Model validation

Effect of convection on extraction rate

The mechanistic model developed in this study has been validated with previous experimental work performed by our group for the extraction of benzene from an aqueous solution by a polydimethylsiloxane (PDMS) coating.¹² The model developed in this study can

predict the equilibration time with the absence or presence of stirring in the sample solution (Figure 2) The equilibration time, 100 seconds, predicted by the present model is in agreement with the experimental data presented in a previous study¹² with stirring speeds as high as 2,500 rpm. Moreover, the simulated results for varying coating thicknesses provided very good fitting with the experimental data, as shown in the supplementary information (Figure S2). The good fitting of the experimental data indicates the coupling between solution and coating phases in the mathematical model both for agitated and non-agitated sample systems.

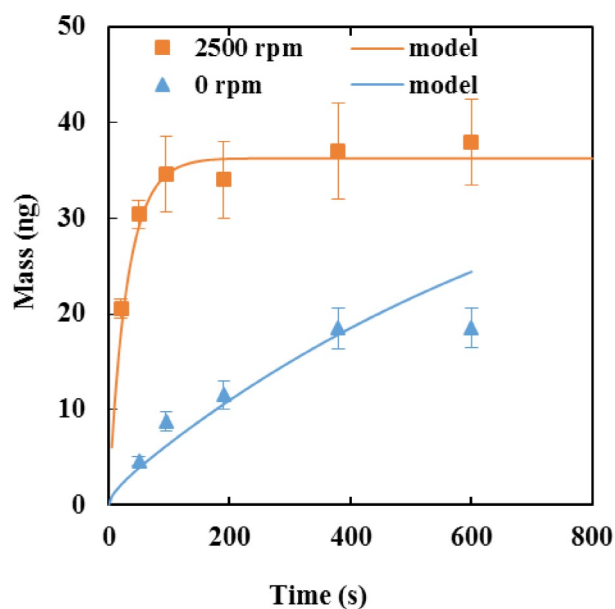


Figure 2. Effect of stirring on the extraction profile of 1 ppm benzene in water extracted with a 56 μm thick PDMS coating Here, D_A^s : $1.08 \times 10^{-9} \text{ m}^2/\text{s}$, D_A^f : $2.8 \times 10^{-10} \text{ m}^2/\text{s}$, C_A^s : $0.0128 \text{ mol}/\text{m}^3$, K_{fs} : 125. The error bars represent standard deviations ($n=3$).

Matrix effect on extraction rate

In SPME, sample matrix can affect the extraction in several ways. For example, binding of analyte to matrix can decrease in measured concentration, especially when high recoveries is desirable for the determination of total concentration. This is due to the reduced amount of

available free analyte to be extracted by SPME fiber due to significant binding of analyte to matrix if depletion is insignificant. Other matrix effects includes the effect of salinity, pH and temperature on the extraction efficiency. The explanation of the abovementioned matrix effects are well accepted by scientific community.⁷ However, the matrix effect on the SPME extraction rate where there is no significant damage of the fiber by physical adsorption/partition of matrix components is still not well explained. While some researchers observed enhanced rates others showed unaltered or reduced rates of extraction. Here, the developed mathematical model is employed to explain the mechanism of the kinetics of extraction in presence of matrix in sample. In the following sections, the “matrix effect” means only the effects on the extraction kinetics. In order to test whether the model can reproduce experimental data for enhanced or unaffected of extraction kinetics, two different experimental set-up was considered. First, the model was validated with experimental data reported by Hermens *et al.* on the effect of bovine serum albumin (BSA) on uptake kinetics of pyrene from an aqueous sample using a PDMS fiber coating.¹⁹ The experimental and simulated data are shown in Figure 3(a). The model predicted the experimental data very well, even at different concentration levels of albumin. In this experimental set-up, the uptake rate was enhanced by the increased concentration of albumin. Another validation of the model is shown in Figure 3(b), with the experimental data obtained from Broeders *et al.*²⁰ The proposed model has been shown to predict experimental data when the rate of uptake was not perturbed while the extracted amount at equilibrium was less in the presence of matrix (albumin) than that of the standard chlorpromazine (analyte) sample. The mechanisms of the different matrix effects on the rate of extraction is discussed in detail in the following sections.

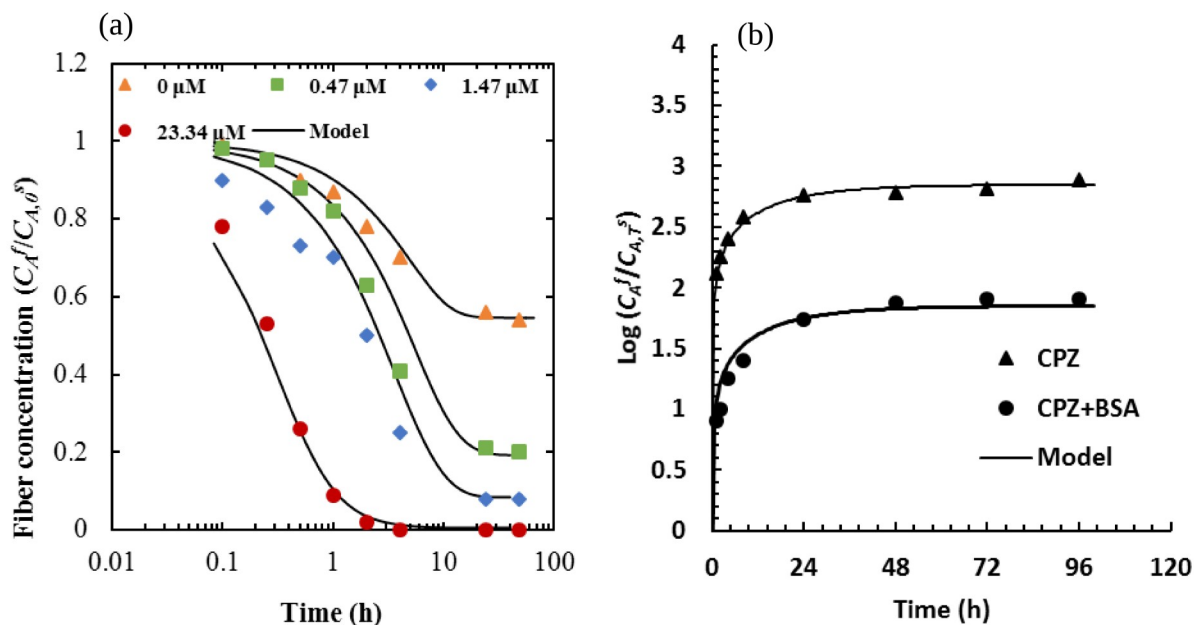


Figure 3. Influence of matrix (albumin) on the rate of extraction. Both the extraction rate and extracted amount were influenced by the presence of albumin in pyrene extraction in PDMS fiber (a). Only the extraction amount was influenced by the presence of albumin in chlorpromazine extraction by polyacrylate coating (b). The experimental and model data are shown in supplementary information (Table S1).

Mechanisms of the matrix effects on uptake kinetics

The literature review indicates that possible matrix effects on SPME kinetics fall into three different categories. The most common is the enhancement of uptake rate, leading to shorter equilibration times. This rate enhancement is particularly problematic when the goal is to measure the freely dissolved concentration under non-equilibrium conditions. In other words, calibration of SPME under non-equilibrium conditions would be possible only if the matrix containing the sample to be analyzed and the calibration sample (without matrix) had identical uptake dynamics. This enhanced rate was typically observed where the amount of extracted analyte by the coating was negligible (usually less than 5%) compared to the initial amount

present in the sample, i.e., the depletion was negligible.⁷ The second class of matrix effect observed was with sampling systems where a significant quantity of analyte was depleted from the sample matrix. While the rate of extraction becomes slower in the matrix-containing sample, the extracted amount is almost the same compared to the matrix-free standard sample.²¹ The third class of matrix effect pertains to an initial fast extraction followed by a slower rate, which increases the equilibration time.²² With the help of an asymptotic analysis,¹¹ these three possible scenarios can be described by the present model, and are explained next.

To explanation of the matrix effects on kinetics, the physical process of transport under the condition of diffusion-limited extraction is described considering the following three dimensionless parameters:

Where α represents the amount of freely dissolved analyte ($C_{A,0}$) at the beginning of the experiment relative to the total amount of matrix ($C_{B,T}$). This term is influenced by the K_D of the analyte-matrix pair, since the system is assumed to be initially at equilibrium; therefore, α represents a measure of the free analyte in the sample matrix. The second parameter, β , relates the timescale of analyte diffusion to the timescale of unbinding of the analyte-matrix complex. This term is dependent on the size of the sample container (L), the dissociation rate of the complex (k_r), and the diffusivity of the analyte through the sample (D_A^s). The third parameter, γ , is the concentration of bound matrix in the sample relative to the unbound portion at the beginning of the experiment. For $\gamma \gg 1$, most of the matrix species are in the bound state

initially. Conversely, if $\gamma \ll 1$, only a small fraction of the matrix has bound analytes. This term is governed by K_D and the amount of free analyte at the beginning of an experiment.

Scenario one: enhanced uptake rate; diffusion controlled kinetics

Effect of K_D on uptake kinetics

At first, the diffusion-controlled kinetics of SPME was established by increasing the diffusivity of the analyte in the solution and observing the concomitant changes in the extraction time profiles (Figure S3, found in supplementary information). An increase in analyte diffusivity in the solution, from 1×10^{-9} to 5×10^{-6} m²/s, yielded a substantially faster uptake rate, which supports the diffusion-controlled kinetics hypothesis. In order to study the effect of different parameters of extraction, an experimental system using chlorpromazine binding to BSA was considered,²⁰ where the equilibrium dissociation constant (K_D) was calculated as 5.4×10^{-4} M. The K_D is a measure of binding strength between the analyte and matrix; generally, the higher the hydrophobicity (higher $\log P$), the lower the K_D value for the analyte albumin complex. Please note that a PDMS coating was assumed instead of using a polyacrylamide coating, as the present scenario aims to study extraction under the diffusion-controlled regime. The mathematical model was used to investigate the effect of K_D on the extraction kinetics, since the kinetics are not sensitive to changes in individual values of k_f and k_r (Figure S4, found in supplementary information). The effect of K_D was studied by varying k_r while keeping k_f constant, since the rate of association tends to be more consistent between binding pairs than the rate of dissociation. Figure 4 shows that the kinetic of extraction is influenced by the strength of the analyte-matrix pair (K_D). Interestingly, K_D values of 10^{-5} and 10^{-6} provided the most significant enhancement in this study. The asymptotic analysis provided that under the condition of diffusion-controlled

kinetics, i.e., fast decomplexation ($\beta \gg 1$), and with a small proportion of bound matrix ($\gamma \ll 1$), extraction occurs over a single time scale (t_s), according to:

$$(15)$$

This term demonstrates that the extraction rate is dependent on the hydrophobicity of the analyte. Increasing hydrophobicity under these conditions will lead to a decrease in equilibration time. The model predicts that a weak interaction (10^{-3} M) does not appreciably affect the diffusional extraction rate (equilibrium reached at 20 minutes), whereas a strong interaction (10^{-6} M) significantly slows the rate of change, with only 5 minutes needed to reach equilibrium. A weak binding partner does not appreciably perturb the kinetics under this condition, although the conditions $\beta \gg 1$ and $\gamma \ll 1$ were pertained in all the cases.

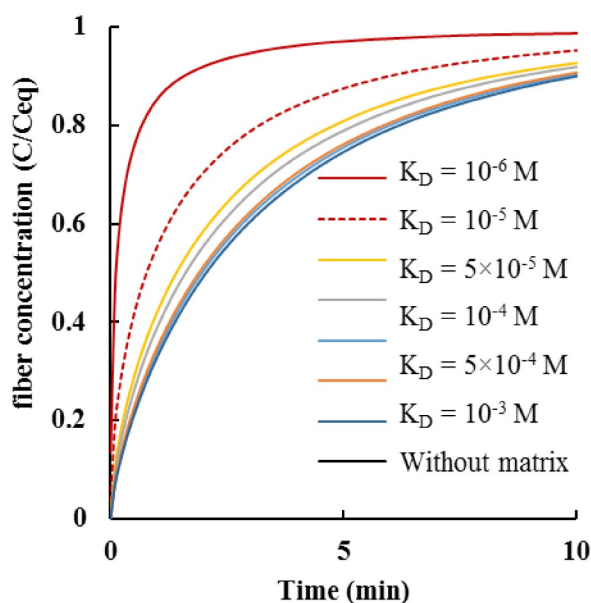


Figure 4. Model simulation of extraction kinetics influenced by varying the strength of the binding matrix from weak ($K_D = 10^{-3}$ M) to strong ($K_D = 10^{-6}$ M), for a chlorpromazine to BSA ratio of 1: 2.5. For this study, k_f was kept constant at $1 \times 10^6 \text{ M}^{-1} \text{ s}^{-1}$ and k_r varied to obtain different K_D values. For all values of k_f and k_r , $\beta \gg 1$ and $\gamma \ll 1$.

Effect of analyte to matrix ratio on uptake kinetics

The mathematical model was used to examine the effect of the initial analyte-to-matrix ratio, containing both weak and strong bindings, on the enhancement of the extraction kinetics. In this case, the analyte concentration was held constant while the matrix concentration was varied. As shown in Figure 5(a), for the weak binding complex system (K_D of 5.4×10^{-4} M), the simulation results show that an increase in analyte-to-BSA ratio of 1:25 to 1:1000 provides a 25 percent enhancement in the kinetics. For the strong binding complex system ($K_D = 5.4 \times 10^{-5}$ M), shown in Figure 5(b), a similar range of enhancement is achieved using an increase in ratio from only 1: 2.5 to 1:100. This phenomenon can be analyzed using the timescale according to equation (15). If , then the rate of extraction is independent of both the matrix concentration and K_D . Therefore, the matrix concentration must be greater than K_D for an enhancement of the uptake rate to occur. In other words, at a lower ratio of analyte to matrix, the rate of extraction is barely affected by the matrix, but the effect becomes pronounced as the ratio increases. Ramos *et al.*²³ reported that the matrix (humic acids) did not interfere with the determination of the freely dissolved concentration of hydrophobic organics under non-equilibrium SPME with a PDMS coating. Oomen *et al.*²⁴ indicated that this observed result might be due to the use of a very low concentration of the matrix in the experiment, which produced a lower concentration of bound matrix than that of free analytes. The present mechanistic model with the asymptotic analysis quantitatively explained the required conditions for influencing the uptake kinetics.

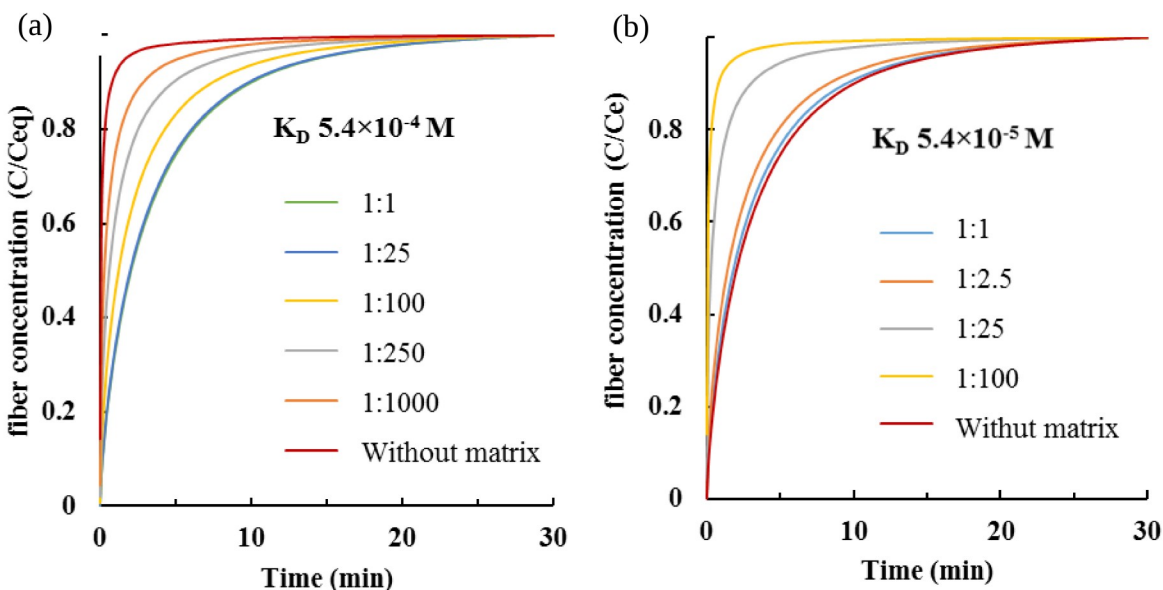


Figure 5. Effect of analyte-to-matrix ratio on the extraction kinetics. Weak binding complex, (a) and strong binding complex (b). The extent of kinetic enhancement is positively influenced by the strength of the binding partners.

Scenario two: retarded uptake rate; diffusion controlled kinetics

A decrease in uptake rate has been observed in cases where the uptake is still controlled by the diffusion of analyte in solution; however, in such cases, the freely dissolved analyte is locally depleted in the diffusion boundary layer due to the extraction by the fiber, i.e., local depletion is significant. Porschmann *et al.* reported a retardation in the uptake rate after addition of humic or fulvic acid to a water sample with organotin compounds, i.e. the time to reach equilibrium was increased.²¹ Similarly, a retardation of uptake kinetics is observed when smaller sample volumes and lower concentrations of analyte are used compared to the capacity of the SPME coating. For instance, Reyes-Garces *et al.* reported slow uptake rates for some moderate hydrophobic compounds (for example, metoprolol) in blood plasma samples.²² This category of matrix effect can be explained by the present asymptotic analysis and the mathematical model. This type of slow kinetics is observed when the kinetics are controlled by diffusion ($\beta \gg 1$) and

when a large proportion of the matrix is bound ($\gamma \ll 1$). A two-stage extraction time profile is obtained with the initial timescale t_s , shown in equation (15), until the analyte concentration is reduced to K_D . The first stage of extraction depends on the total matrix concentration and the initial free analyte concentration. As the free concentration is depleted, the second stage of extraction starts with a timescale matching the one shown in previous section. for the remaining analyte molecules present in the sample. Figure 6 compares the effect of the matrix on the uptake kinetics under the abovementioned condition by using the developed model. For the extraction time profile of matrix containing sample, Figure 6 an initial fast extraction is followed by slow diffusion-controlled conditions. Therefore, the mathematical model presented here can be used to predict uptake profiles in cases where the rate is retarded by the local depletion of analyte, but where the kinetics are still diffusion-controlled.

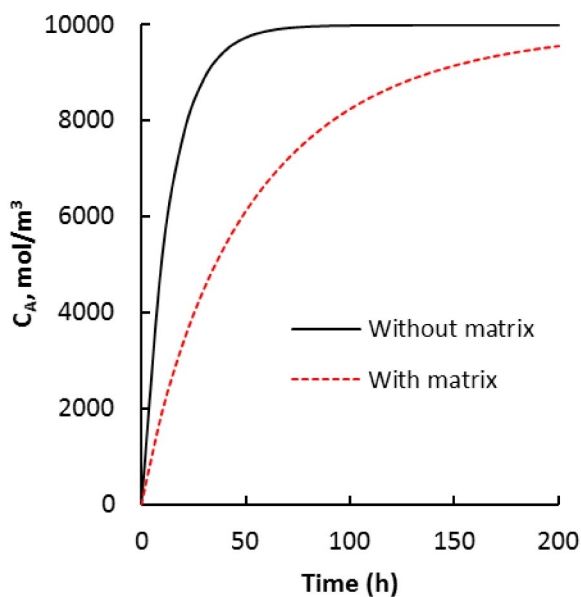


Figure 6. Retardation of uptake kinetics in the presence of matrix. Extraction time profiles in pure water without the addition of matrix (solid line, black) and with the addition of matrix (dashed line, red). Parameters are shown in Table S2.

Scenario three: retarded uptake rate; analyte dissociation-controlled kinetics

In the third case, the matrix substantially reduces both the uptake rate and the extraction amount at equilibrium. This type of profile was recently reported by Reyes-Garces *et al.* for the extraction of a very hydrophobic analyte, stanozolol (K_D with HSA = 5 nM) from a blood plasma sample.²² From the mathematical analysis and computational simulation, the condition for this scenario is that the dissociation of bound analyte from the matrix is slow compared to the diffusion in solution, i.e., $\beta \ll 1$ or . Any free analyte produced by dissociation of the analyte-matrix pair is negligible compared to the existing freely dissolved analytes in the sample solution. As shown in Figure 7, nearly all the freely dissolved analyte is extracted by the coating over the diffusion timescale, L^2/D_A^s . The initial fast diffusive uptake is followed by the slow dissociation of bound analytes over the timescale of $1/k_r$. Since analyte diffusivity through environmental or biological samples does not change significantly, either k_r or L needs to be modified for our computational sample system to observe this type of slow kinetics. It is more feasible to modify the diameter of the sample container than the binding kinetics. If the diameter is kept constant at 10 mm, as in the previous simulation experiments, a k_r of $< 10^{-4} \text{ s}^{-1}$ is required for $\beta \approx 1$. This translates to a bound matrix with a half-life of ~ 3 hours. However, if the vial diameter is sufficiently decreased, it is possible to achieve $\beta \ll 1$ for physically relevant k_r values. More precisely, in order to observe the unbinding-controlled dynamics, the diameter L would need to be below the order of . It was also found that the slower uptake rate is dependent on the extraction capacity of the coating (K_{fs}) when the value of k_r is kept constant (Figure S5, found in the supplementary information).

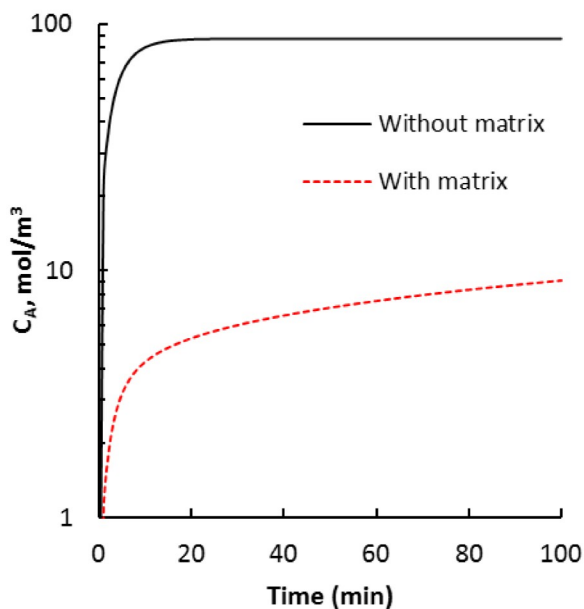


Figure 7. Retardation of uptake kinetics, which is controlled by dissociation of analyte from the bound matrix. Extraction time profile in the absence of matrix (solid line, black) and in the presence of matrix (dashed line, red).

The information provided by the above analysis can be used to design an experimental set-up with desired extraction time profiles. In the first scenario, the rate of analyte extraction decreases smoothly over a single timescale. In the other two cases, there are two distinct timescales: an initially fast uptake rate, followed by a more gradual uptake rate. The two timescales in the second case are related, as they are both proportional to L^2/D_A^s , whereas the two timescales in the third case are independently controlled by L^2/D_A^s and k_r , as long as $\alpha \gg \beta\gamma/(\gamma+1)$ and . Another key difference between the last two cases is that all of the bound analyte molecules remain in the bound state throughout the fast mode for the third case, while approximately half of the bound analyte molecules undergo unbinding in the initial fast stage for the second case. Thus, the complex sample system can influence not only the timescales of extraction, but also by the amounts of analyte extracted in each stage.

Conclusions

The current work presented a mechanistic-based mathematical model that describes the uptake kinetics in SPME for analytes either from a standard solution or a matrix-containing solution. The proposed mathematical model provided excellent prediction of the experimental data available in the literature. The uptake kinetics process under no-equilibrium extraction conditions was previously an obscure area of discussion. It was not clear under what experimental conditions the uptake rate is altered with the presence of binding matrix in sample solution. Now, with the help of this mathematical model and computational simulation, one can easily determine whether the matrix will enhance or retard the uptake kinetics based on the physicochemical properties of the analyte, the matrix, as well as the choice of SPME coating. Overall, the simulation results obtained for the present analysis have shown that the present model is a reliable and relatively inexpensive practical method of characterizing the performance of SPME. This model can be used for sample matrices containing one type of undesirable components. However, for biomedical application such as human blood or tissue sampling with SPME, further improvement of the model describing the multicomponent phenomena is needed. We are currently extending this study to the application of SPME extraction in tissue or blood sampling.

Acknowledgments

This work was supported by the Natural Sciences and Engineering Research Council of Canada and the Premier Discovery Award. The authors are thankful for initial suggestions on this project from Wennan Zhao and Zhipei Qin from the Department of Chemistry at the University of Waterloo.

Supporting Information

Parameters used for fitting experimental data, coating/solution interface boundary conditions, Effect of coating thickness on kinetics, test for boundary layer controlled diffusion, effect of binding rate constants and partition constants on uptake kinetics.

Nomenclature

Symbol	Name
M	Stiff-spring velocity
C_A^s	Analyte concentration in solution
K_f	Association rate constant
K_r	Dissociation rate constant
K_{fs}	Partition coefficient
D_A^s	Diffusion coefficient of analyte in solution
D_A^f	Diffusion coefficient of analyte in fiber
C_B	Bound analyte concentration
D_{BS}	Diffusion coefficient of the complex in solution
B	Diameter of the fiber core
A	Thickness of the fiber coating
P	Density of water
μ	Dynamic viscosity of water
R	Radius of the magnetic stirrer
L	Radius of the sample container

References

1. Boyaci, E.; Rodriguez-Lafuente, A.; Gorynski, K.; Mirnaghi, F.; Souza-Silva, E. A.; Hein, D.; Pawliszyn, J. *Anal. Chim. Acta* **2015**, *873*, 14-30.
2. Pawliszyn, J. *solid phase microextraction: theory and practice*. Wiley-VCH: Toronto, 1997.
3. Lao, W.; Maruya, K. A.; Tsukada, D. *Anal. Chem.* **2012**, *84*, 9362-9369.
4. Eijkeren, J. C.; Heringa, M. B.; Hermens, J. L. M. *Analyst* **2004**, *129*, 1137-1142.
5. Vaes, W. H. J.; Ramos, E. U.; Casper, H.; Holsteijn, I.; Blaauboer, B. J.; Seinen, W.; Verhaar, H. J. M.; Hermens, J. L. M. *Chem. Res. Toxicol.* **1997**, *10*, 1067-1072.
6. Heringa, M. B.; Hogevoender, C.; Busser, F.; Hermens, J. L. M. *J. Chromatogr., B: Anal. Technol. Biomed. Life Sci.* **2006**, *834*, 35-41.
7. Heringa M.B. , Hermens. J. L. M. *Trends Anal. Chem.* **2003**, *22*, 575-587.
8. Kopinke, F. D.; Ramus, K.; Poerschmann, J.; Georgi, A. *Environ. Sci. Technol.* **2011**, *45*, 10013-10019.
9. Heringa, M. B.; Pastor, D.; Algra, J.; Vaes, W. H. J.; Hermens, J. L. M. *Anal. Chem.* **2002**, *74*, 5993-5997.

10. Santillo, M. F.; Ewing, A. G.; Heien, M. L. *Anal. Bioanal. Chem.* **2011**, 399, 183-190.
11. Vulic, K.; Pakulska, M. M.; Sonthalia, R.; Ramachandran, A.; Shoichet, M. S. *J. Controlled Release* **2015**, 197, 69-77.
12. Louch, D.; Motlagh, S.; Pawliszyn, J. *Anal. Chem.* **1992**, 64, 1187-1199.
13. Mahmud, T.; Haque, J. N.; Roberts, K. J.; Rhodes, D.; Wilkinson, D. *Chem. Eng. Sci.* **2009**, 64, 4197-4209.
14. Bird, R. B.; Stewart, W. E.; Lightfoot, E. N. *Transport Phenomena*. 2nd ed.; Wiley & Sons: Toronto, 2002.
15. Datta, A.; Rakesh, V. *An Introduction to Modeling transport processes*. 1st ed.; Cambridge University Press: New York, 2010.
16. Buchwald, P. *Theor. Biol. Med. Model.* **2009**, 6, 5.
17. Ellis, J. S.; Strutwolf, J.; Arrigan, D. W. *Phys. Chem. Chem. Phys.* **2012**, 14, 2494-500.
18. Crank, J. *The Mathematics of Diffusion*. 2nd ed.; Clarendon Press: Oxford, 1975.
19. Kramer, N. I.; Eijkeren, J. C. H.; Hermens, J. L. M. *Anal. Chem.* **2007**, 79, 6941-6948.
20. Broeders, J. J.; Blaauboer, B. J.; Hermens, J. L. M. *J. Chromatogr., A* **2011**, 1218, 8529-8535.

21. Poerschmann, J.; Zhang, Z.; Kopinke, F. D.; Pawliszyn, J. *Anal. Chem.* **1997**, *69*, 597-600.
22. Reyes-Garces, N.; Bojko, B.; Pawliszyn, J. *J. Chromatogr., A* **2014**, *1374*, 40-49.
23. Ramos, E. U.; Meijer, S. N.; Vaes, W. H. J.; Verhaar, H. J. M.; Hermens, J. L. M. *Environ. Sci. Technol.* **1998**, *32*, 3430-3435.
24. Oomen, A. G.; Mayer, P.; Tolls, J.; *Anal. Chem.* **2000**, *72*, 2802-2808.

For TOC only

